ANNUAL REPORT 2012-13

UNIVERSITÀ DEGLI STUDI DEL PIEMONTE ORIENTALE "AMEDEO AVOGADRO"

DOCTORATE (PH.D.)

IN

MOLECULAR MEDICINE XXVII CYCLE

Candidate

Aastha Jindal

Tutor

Prof. Emanuele Albano

Contents

Introduction

Nonalcoholic fatty liver disease (NAFLD) and nonalcoholic Steato-hepatitis (NASH) form a spectrum of disease characterized by accumulation of excess fat within (steatosis) the liver variously associated with lobular inflammation parenchymal injury and fibrosis [1,2]. They are considered as the hepatic manifestations of the so called 'Metabolic Syndrome' a cluster of closely related clinical features linked to visceral obesity that include insulin resistance, dyslipemia and cardiovascular diseases. NAFLD/NASH is now the most frequent hepatic lesion in western countries with prevalence in the general population ranging from 3-15% but reaching up to 70% among overweight individuals [1,3]. While simple steatosis in NAFLD is most often benign, in about 20-30% of patients the disease can progress to NASH, a condition characterized by hepatocellular damage, intralobular inflammation and fibrosis that not rarely, leads to liver cirrhosis and in some case to hepatocellular carcinoma [4]. In fact, within 8 years, 15% of NASH patients develop clinically and histologically evident cirrhosis. Death rate ascribed to NASH-related cirrhosis accounts for 12-25%, while end-stage NASH is responsible for about 4-10% of liver transplants. A further matter of concern in NAFLD/NASH epidemiology is its increasing diffusion among children and adolescents as consequence of the growing of childhood obesity and overweight [5]. NAFLD prevalence among children and adolescents ranges between 2.6% and 9.8% respectively and is especially high among obese subjects, making it the most frequent pediatric chronic liver disease all over the world. The clinical and social relevance of NAFLD/NASH has stimulated a number of studies to clarify the mechanisms leading to the disease in an attempt to develop effective treatments. However, the mechanisms responsible for the progression of NAFLD to more severe liver injury remain poorly understood.

Studies in patients and in experimental models of NASH suggest that oxidative stress and metabolic alterations may play a role in the progression of disease [6]. FFA and cholesterol accumulation within the mitochondria along with TNF-α cause mitochondrial dysfunction and increase reactive oxygen species (ROS) generation. In turn, ROS-dependent lipid peroxidation promotes a self-sustaining loop that leads to further mitochondrial damage and causes mitochondrial DNA (mtDNA) mutations [7-9]. Increased production of reactive nitrogen species (RNS) generated as a consequence of nitric oxide synthase 2 (NOS2) induction by pro-inflammatory cytokines also contributes to oxidative injury [10]. Accordingly, a significant increase of oxidative damage markers along with a concomitant reduction of the liver antioxidant content is evident in NAFLD/NASH patients. Excess liver uptake of FAA also promotes endoplasmic reticulum (ER) stress and lipotoxicity by activating a variety of stress-responsive kinases, including c-Jun N-terminal kinases 1/2 (JNK1/2) [11-13]. On their turn, oxidative stress, ER stress, mitochondrial dysfunctions and JNK1/2 activation may further promote hepatic insulin resistance, favour hepatocyte death. Inflammation, along with hepatocyte damage, is the main feature of the progression from simple steatosis to NASH. In fact, the molecular mechanisms able to promote inflammation cross-talk with those responsible for hepatocellular damage and fibrosis [13,14]. In this context, the oxidative stress within parenchymal cells stimulates NF-κB-mediated production of TNF-à and IL-6 by hepatocytes [14,15]. In turn, these cytokines stimulate Kupffer cells to secrete inflammatory mediators, which recruit to the liver phagocytic cells. Pattern-recognition receptors, including Toll-like receptors (TLRs), contribute to the pro-inflammatory responses in fatty livers. TLR-responses can be activated by apoptotic cell death, hypoxia/HIF, and inflammation [16,17]. TLR stimulation activate NF-κB, and thereby further amplify and sustain inflammatory signals. Consistently, NASH patients show an

increased hepatic expression of cytokine genes that correlates with the severity of liver lesions [16,18]. Moreover, interference with NF-κB activation protects significantly from the development of steatohepatitis and reduces the expression of TNF-α and intercellular adhesion molecule-1 in rodent models of NASH [19,20].

As a result of unresolved inflammation the liver undergoes to pathologic repair, thus progressive fibrosis and cirrhosis represent the final outcomes of NASH. NASH-related fibrosis develops primarily in the pericentral areas, where thin bundles of fibrotic tissue surround groups of hepatocytes and thicken the space of Disse, in a "chicken wire" fashion. The main cell type responsible for extracellular matrix deposition are hepatic stellate cells (HSCs), which under the local influence of transforming growth factor β1 (TGF-β1), platelet-derived growth factor (PDGF) and MCP-1 trans-differentiate into myofibroblast-like cells (HSC/MSs) producing collagen and extracellular matrix components [21,22]. Furthermore, decreased hepatic matrix degradation due to a reduced production of matrix metalloproteases (MMPs) and/or an increased production of matrix metalloproteases inhibitors might also contribute to collagen accumulation [23,24]. Kupffer cell activation in response to chronic inflammatory stimuli is mostly responsible for the secretion of pro-fibrogenic cytokines [25,26].

A further mechanism by which oxidative stress can stimulate inflammation involves adaptive immunity. Indeed, the interaction of lipid peroxidation products with cellular proteins leads to the formation of immunogenic adducts that induce both humoral and cellular immune responses. Data emerging from experimental models of atherosclerosis indicate that IFN-γ, TNF-α, and CD40 ligand (CD154) produced by Th-1 CD4+ T-cell responsive to antigens in oxidized LDL, drive plaque macrophages to produce reactive oxygen species, NO, and proinflammatory cyto/chemokines. In line with these findings, previous studies from our laboratory have shown that high titers of IgG against some of the antigens originating from oxidative stress, namely malondialdehyde- (MDA) derived adducts, are detectable in about 40% of adult NAFLD/NASH patients and in 60% of children with NASH [27]. In these latter, high antibody titers are an independent predictor of fibrosis, while in pediatric NASH anti-MDA IgG associated with more severe lobular inflammation and a 13 fold increased risk of severe disease [27].

From this background, we sought to investigate the possible contribution of immune reactions triggered by oxidative stress in modulating hepatic inflammation in NASH. To this aim, we have taken advantage from an animal model of NASH involving mouse feeding with a methionine/choline deficient (MCD) diet that allow to obtain in a reproducible manner steatohepatitis similar to human NASH after 3-4 weeks of treatment or steatohepatitis plus fibrosis by extending the treatment up to 8-10 weeks.

Materials & Methods

Animals and Experimental protocol.

Eight weeks old male C57BL/6 mice were purchased from Harlan-Nossan (Corezzana, Italy) and fed for 4 or 8 weeks with either methionine-choline deficient (MCD) or control diets (Laboratorio Dottori Piccioni, Gessate, Italy). For immunization experiments mice were injected subcutaneously with 100μg of MDA-adducted bovine serum albumin (MDA-BSA) in incomplete Freud's adjuvant and re-boosted after one week with the same antigen. The control

groups received either saline or incomplete Freud's adjuvant injections. MCD diet feeding was started 2 weeks after the second injection. In some experiments immunized mice were treated with the anti-CD4 monoclonal antibody GK1.5 (BioXCell, West Lebanon, NH, USA) while receiving the MCD diet to deplete hepatic CD4+ T cells (See supplementary materials for further details). The efficiency of cell depletion was preliminary evaluated by flow cytometry in the liver and the spleen and was >97%. All the experiments were approved by the Italian Ministry of Health and by the University Commission for Animal Care following the criteria of the Italian National Research Council.

Biochemical analysis

Plasma ALT and liver triglyceride were determined by spectrometric kits supplied by Radim S.p.A. (Pomezia, Italy) and Sigma Diagnostics (Milano, Italy), Liver osteopontin content was evaluated by a commercial ELISA kit supplied by R&D Systems (Abingdon, UK).

Antigen preparation and antibody measurement.

Protein adducts with lipid peroxidation products were prepared as in [28] and used to coat polystyrene microwell ELISA plates (Nunc, S/A, Roskilde, Denmark) . Mouse sera (0.20 ml, 1:50 dilution) were added in duplicate and the antibody binding was revealed using peroxidase-linked goat anti-mouse IgG or IgM sera as previously described [28]. The results were expressed as optical density following the subtraction of background reactivity.

mRNA extraction and Real time PCR

Liver RNAs were retro-transcripted with High Capacity cDNA Reverse Transcription Kit (Applied Biosystems Italia, Monza, Italy). RT-PCR was performed in a Techne TC-312 termalcycler (TecneInc, Burlington NJ, USA) using TaqMan Gene Expression Master Mix and TaqMan Gene Expression probes for mouse TNF-α, IL-12p40, IL-17a, RORγT, IFN-γ, T-bet, CCL2, iNOS, CD40, CD40L, osteopontin, α1-procollagen, and beta-actin (Applied Biosystems Italia, Monza, Italy). All samples were run in duplicate and the relative gene expression was calculated as $2^{-\Delta Ct}$ over that the house keeping β-actin gene. The results are expressed as fold increase over the control samples.

Histology and Immunohistochemistry

Liver pathology was assessed in hematoxylin-eosin and Masson's trichrome stained sections. Steatosis and lobular inflammation were scored blind by an experienced pathologist (C.B.) according to Kleiner et al [29]. The number of necro-inflammatory foci were counted in ten different high magnification microscopic fields. Hepatic macrophages were evidenced in formalin-fixed sections using, respectively, anti-mouse F4/80 (eBioscience, San Diego CA, USA) in combination with peroxidase-linked goat anti-rat IgG and horse-radish peroxidase polymer kit (Biocare Medical, Concord, CA, USA).

Intrahepatic lymphocyte isolation and flow cytometry analysis

Hepatic mononucleated cells were isolated and purified on a density gradient as in [30]. The cells were stained with fluorochrome-conjugated antibodies for CD45, CD3, CD4, CD8, CD69, CD107a, IL-2 and IFN-γ (eBiosciences, San Diego CA, USA) and analyzed with a FACScalibur

(Becton Dikinson) flow cytometer. De-complemented mouse serum was used to block unspecific immunoglobulin binding. A polyclonal anti-osteopontin rabbit antiserum (Millipore, Temecula, CA, USA) and phycoerythrin-conjugated anti-rabbit IgG (Sigma-Aldrich, Milan, Italy) were used for detecting ostepontin producing cells. The response of intra-hepatic lymphocytes to MDA adducts was investigated following an overnight incubation with MDA-adducted or native murine albumin (10µg/mL) in the presence of brefeldin A (3µg/ml), anti-CD3e and CD28 antibodies (1µg/ml) by detecting IL-2 producing cells with flow cytometry [31].

Data analysis and statistical calculations

Statistical analyses were performed by SPSS statistical software (SPSS Inc. Chicago IL, USA) using one-way ANOVA test with Tukey's correction for multiple comparisons or Kruskal-Wallis test for non-parametric values. Significance was taken at the 5% level. Normality distribution was preliminary assessed by the Kolmogorov-Smirnov.

Results

Effects of MCD diet on liver transaminases, triglycerides and oxidative stress in mice

The pathological consequences of NASH can be reproduced in mice by feeding a methionine/choline deficient (MCD) diet [32]. As shown in Fig.1, C57BL/6 mice fed with MCD diet for up to eight weeks showed a progressive increase in serum alanine aminotransferase (ALT) levels and accumulation of triglycerides within the hepatocytes. Histological examination demonstrated that macrovesicular steatosis involving lobular zones 2/3 was evident after 4 weeks of the MCD diet, as shown in Fig.2. Panlobular steatosis developed in later stages with the increase in the degree of fat accumulation. Oxidative stress, as measured by thiobarbituric acid reactive compounds (TBARs) in Fig.1, was also evident in these animals and hepatic TBARs concentrations increased by respectively 50–80% after 4 and 8 weeks of treatment.

MCD diet induced development of hepatic inflammation

Beside parenchymal injury steatohepatitis is characterized by inflammatory damage in liver. As shown in Fig.2, at histology moderate focal lobular inflammation was evident at 4 weeks and further increased thereafter when an intense panlobular and portal chronic inflammatory infiltrate was evident. Necro-inflammatory infiltrates were also highly evident from the early stages and further advanced in later stages of the disease. The onset of inflammation was prominently depicted in the rising levels of inflammatory mediators like TNF-α and CCL2 with over 8-10 fold increase from 4 weeks to 8 weeks of MCD diet which was completely evidential to the histological observed in the tissue sections.

Involvement of oxidative stress related antigens in humoral and cell-mediated immune responses

As in humans, oxidative stress was associated with the development of IgG against adducts originating from lipid peroxidation products, such as malonyldialdehyde (MDA) and 4-hydroxynonenal (4-HNE) and the individual IgG reactivity against MDA-adducts, but not liver TBARs, positively correlated with ALT release and hepatic TNF-α mRNA expression ($r=0.61$, $p=0.04$; $r=0.66$, $p=0.03$, respectively), as shown in Fig.1. Immunohistochemistry of NASH livers revealed that hepatic inflammatory infiltrates were also enriched by T- and B-lymphocytes, the

number of which positively correlated with the individual IgG reactivity against MDA-adducts (r=0.68, p=0.02; r=0.75, p=0.006, respectively) as seen in Fig.3. Fig. 3 shows detailed flow cytometry analysis of hepatic mononucleated cells confirmed a progressive recruitment of T-lymphocytes in NASH livers that involved effector $CD8^+$ T-cells and $CD4^+$ helper T-cells. Furthermore, the proportion of $CD3^+$ T-cells expressing the CD69 activation marker was higher in the livers of MCD-fed mice as compared to controls. Intra-hepatic $CD4^+$ T-cells from mice with NASH also showed an enhanced interferon-γ (IFN-γ) expression. We also observed that $CD8^+$ and $CD4^+$ T-cells obtained from NASH, but not from healthy livers, produced IL-2 when incubated "in vitro" with MDA-modified murine albumin, indicating that lipid peroxidation-derived antigens might contribute to the development of cell-mediated immune responses, which on their turn might contribute to NASH progression.

Immunization against MDA-adducts can alter the severity of NASH in mice

In order to substantiate the possible role of adaptive immunity in promoting hepatic inflammation in NASH, we stimulated immune reactions against MDA adducts by injecting mice with MDA-modified bovine serum albumin (MDA-BSA) in incomplete Freund's adjuvant before the administration of the MCD diet. In our preliminary experiments control diet, we compared liver morphology and function of immunized mice fed with a control diet with that of naïve untreated mice. The histological profile of immunized mice was not different that of its naïve counterparts. In addition, immunization alone did not alter the transaminase activity, liver triglycerides or the hepatic mRNA expression of inflammatory mediators like TNF-α or CCL2. With this reference, we went on feeding the MCD diet to mice which were prior injected with MDA-modified bovine serum albumin (MDA-BSA) plus incomplete Freund's adjuvant or the adjuvant alone. Following four weeks on the MCD diet, ALT release and the hepatic mRNA expression of TNF-α and CCL2 were higher in MDA-BSA-immunized than in naïve mice. No appreciable changes in liver injury and inflammation were observed in mice injected with incomplete Freund's adjuvant before receiving the MCD diet. The enhanced severity of NASH was further supported by histology that showed higher scores for lobular inflammation and an increased number of necro-inflammatory foci and apoptotic cells in MCD-fed immunized mice. Furthermore, these later had several fold rise in transaminase release and liver mRNA content of TNF-α and CCL2 as compared to non-immunized MCD treated mice. Accordingly, circulating levels of TNF-α were three fold higher in MCD-fed immunized mice than in similarly treated naïve mice.

Characterization of immune response associated with the development of NASH in immunized mice.

The observation that the patho-physiological manifestations of MCD diet induced NASH can be worsened by prior MDA-BSA immunization prompted us to further investigate the mechanisms possibly involved. Flow cytometry of intrahepatic lymphocytes showed that MDA-BSA immunization did not modify the liver T-cells profile in mice receiving the control diet. On the contrary, immunization further promoted the recruitment of CD3+ T-cells in MCD-fed mice, increasing both the CD8+ and CD4+ pools. However, the proportion of CD8+ T-cells expressing the CD107a activation marker was unchanged. Th-1 and Th-17 activation of CD4+ T-lymphocytes are regarded as important pro-inflammatory stimuli. We observed that the expression of the Th-1 transcription factor T-cell T-box transcription factor (T-bet) as well as the liver IFN-γ content were selectively increased in MCD-fed immunized animals, in parallel with a

stimulation of macrophages M1 activation markers IL-12p40 and inducible NO synthase (iNOS). Among immunized MCD-fed mice there was also a positive correlation between the individual expression of IFN-γ and that of TNF-α, IL-12p40 and iNOS (r=0.82, 0.75 and 0.88 respectively; $p<0.02$). No changes were instead evident in the hepatic mRNAs for the Th-17 transcription factor retinoic acid-related orphan receptor-γt (ROR-γt) and IL-17a (not shown). Furthermore, MCD-fed immunized mice also showed up-regulated mRNAs for CD40 ligand (CD40L; CD154) and its receptor CD40, a pair of co-stimulatory receptor-ligand molecules involved in macrophage activation by CD4+ T-cells [33]. To further verify the role CD4+ T-lymphocytes in promoting NASH, MCD-fed immunized mice were depleted of CD4+ T-cells by injecting them with the anti-CD4 monoclonal antibody GK1.5 receiving the MCD diet during 4 weeks. In preliminary experiments we observed that the efficiency of CD4+ cell depletion in the liver, as evaluated by flow cytometry, was >97%. Figure ?? shows that following CD4+ T-cell depletion the hepatic mRNA expression of IFN-γ and CD40L as well as that of the macrophage M1 markers iNOS and IL-12p40 were lowered as compared to untreated animals. Histology in these animals also confirmed an improvement of lobular inflammation and focal necrosis.

Discussion

Latest research reports the involvement of adaptive immunity, promoting fat inflammation in obesity, since CD4+/CD8+ T-cells are recruited into the adipose tissue and provide stimulation for the macrophage production of pro-inflammatory mediators [34,35]. Lymphocytes are often detected in the lobular infiltrates of NASH [36], but the actual role of adaptive immunity in the pathogenesis of the disease is still poorly understood. We previously reported that sub-sets of adult and pediatric NAFLD/NASH patients show antibody responses against oxidative stress-related antigens, such as MDA-derived adducts, that associate with an increased severity of lobular inflammation or fibrosis [27,37]. Similar antibodies are also detectable in rats with NASH induced by enteral nutrition with a high fat diet, while preventing oxidative stress with N-acetylcysteine attenuates both the IgG formation and the severity of Steatohepatitis. In the present study, we observed that the progression of NASH caused a methionine/choline deficient (MCD) diet parallels with the development of IgG against lipid peroxidation-derived adducts and the liver recruitment of CD4+ and CD8+ T-lymphocytes recognizing the same antigens. The possible contribution of adaptive immunity to the progression of experimental NASH is further substantiated by the observation that stimulating immune responses against MDA-protein adducts, one of the antigens recognized by the antibodies detected in both human and rodent NASH, promotes parenchymal injury and inflammation in mice fed with the MCD diet. In accord with our observation a recent study by Henning and coworkers has reported that an expansion in the number of hepatic dendritic cells (DCs) characterizes NASH progression in mice receiving the MCD diet. These DCs show increased expression of maturation and activation markers indicating that they are functionally active as professional antigen presenting cells to initiate adaptive responses and in regulating inflammation through production of soluble mediators. Accordingly, DCs from NASH livers exhibit an increased ability to induce allogeneic T-cell stimulation and in particular they promote antigen restricted CD4+ T-cell proliferation, as well as CD4+ T-cell production of T-helper cell Th1, Th2 and Th17 cytokines. NASH DCs also down-regulate expression of the CD25+ FoxP3+ regulatory T-cell (Treg) phenotype in DC/T-cell co-culture experiments to a greater extent than control DCs. However, DC activation of antigen-restricted CD8+ T cells remains unchanged in NASH. In particular, peptide-pulsed

control and NASH DCs induce comparable antigen restricted CD8+ T cell proliferation and cytokine production.

In a recent paper Bieghs and co-workers reported that inducing the production of IgM targeting oxidized low density lipoproteins (LDLs) reduce NASH in LDL receptor-deficient mice receiving a high-fat/cholesterol diet. Our data are not in contrast with these observation and the discrepancies can be explained considering that the experimental settings are quite different for the immune responses involved and the mechanisms leading to NASH. In Bieghs's work mice were immunized with heat-inactivated pneumococci leading to the production of natural IgM against bacterial antigens that cross-react with oxidized phosphatidylcholine in LDLs [38]. Feeding a high-fat/cholesterol diet to LDL receptor-deficient mice causes Kupffer cell engulfment by oxidized LDLs that, in turn, promotes Kupffer cell activation and hepatic inflammation [39]. In this scenario, the IgM interaction with oxidized LDLs reduces their uptake by Kupffer cells, lowering the pro-inflammatory stimuli [39]. These conditions are quite different from those occurring in MCD-induced NASH, where parenchymal injury, oxidative stress and inflammation result from the impairment of hepatocyte lipid secretion [32]. Furthermore, our data indicate that the immunization with MDA-adducts mainly stimulates IgG production and T-cell responses and that these latter are mainly responsible for promoting inflammation.

Concerning the mechanisms by which adaptive immunity contributes the evolution of NASH, we have observed that hepatic CD4+ T-cells are increased in MCD-fed immunized mice in parallel with stimulation in the liver expression of IFN-γ and CD40L (CD154). CD40L is a co-stimulatory molecule predominantly expressed by CD4+ T-cells and activated platelets that, by interacting with its receptor CD40 on macrophages and lymphocytes, have a key role in orchestrating inflammation and immunity in several diseases, including atherosclerosis and obesity [40,41]. In line with this, CD4+ T-cell depletion prevents the up-regulation of IFN-γ and CD40L and ameliorates lobular inflammation, indicating that a Th-1 activation of CD4+ T-lymphocytes plays a major role in promoting NASH. It is noteworthy that Th-1 activation characterizes CD4+ T-cell responses to LDL-derived oxidation antigens in atherosclerosis [40]. In this setting, CD4+ T cell or IFN-γ deficiency have been shown to ameliorate plaque inflammation and the disease progression [40]. Interestingly, an increase in circulating IFN-γ-producing CD4+ T-cells has been observed in either pediatric or adult NASH patients in conjunction with an enhanced liver IFN-γ production [42], suggesting the possible relevance of these mechanisms to the human disease. A recent report indicates that an increase in hepatic CD8+ T-cells also characterizes pediatric NASH. In our hands, CD8+ T-cell recruitment is evident in NASH livers and is further promoted by pre-immunization [42]. However, immunization does not affect the expression CD8+ T-cell activation markers, suggesting that in our experimental setting effector T-cells do not significantly contribute to hepatic inflammation. Nonetheless, the involvement of CD8+ T-cells in NASH requires further investigations. In a similar manner, more studies are needed to clarify the role of B-cell responses. Indeed, the presence of circulating anti-MDA IgG might not be just a hallmark of immune activation against oxidative stress derived epitopes, but might influence the disease evolution by causing antibody-mediated injury. Furthermore, B-cells have been shown to drive CD4+ T-cell activation and cytokine production in the adipose tissue during obesity and either stimulate or prevent the progression of liver injury to fibrosis [43,44].

In conclusion, the results presented indicate that immune responses triggered by oxidative stress-derived antigens contribute to hepatic inflammation in experimental NASH by promoting the Th-1 activation of CD4+ T-lymphocytes. Altogether, these data support recent observations in humans about the possible involvement of adaptive immunity in the mechanisms leading to NAFLD evolution.

Future Prospects

Using the animal model of NASH, it is now clear that the disease severity can be elevated experimentally using prior immunization techniques. Thus, the involvement of adaptive immunity towards in the progression of NASH needs to be studied in much detail by evaluating how the activation of $CD4^+$ and $CD8^+$ T-lymphocytes in the hepatic environment leads to the eventual state of the disease. In this respect it is important to study the behavior of these T-cell subsets during liver damage. In this direction, it is important to measure the activity of these cells at different stages on the disease in an experimental model. We will employ flow cytometry analysis on prior immunized animals, later fed on MCD diet to induce NASH. It is important to understand the path followed by the $CD4^+$ and $CD8^+$ subsets. Also it will be wise to haw depletion of $CD8^+$ T cells with specific antibodies modulates the disease progression. With all this data in hand, still the role of B-cell response remains poorly characterized. A further aim of my project will concern the characterization of the actual relation between B-cell and $CD4^+$ T-cell activation. In this direction, we plan to investigate the B-cell activation and progression profile in the hepatic environment in relation to the $CD4^+$ and $CD8^+$ T-cell population in its vicinity. Experiments will be carried out to understand the humoral immune response during the NASH progression in unison with the cell-mediated immune response. This will help to understand the in whole immune activity which leads to the destruction of hepatic tissue during NASH progression.

Figures

Figure 1

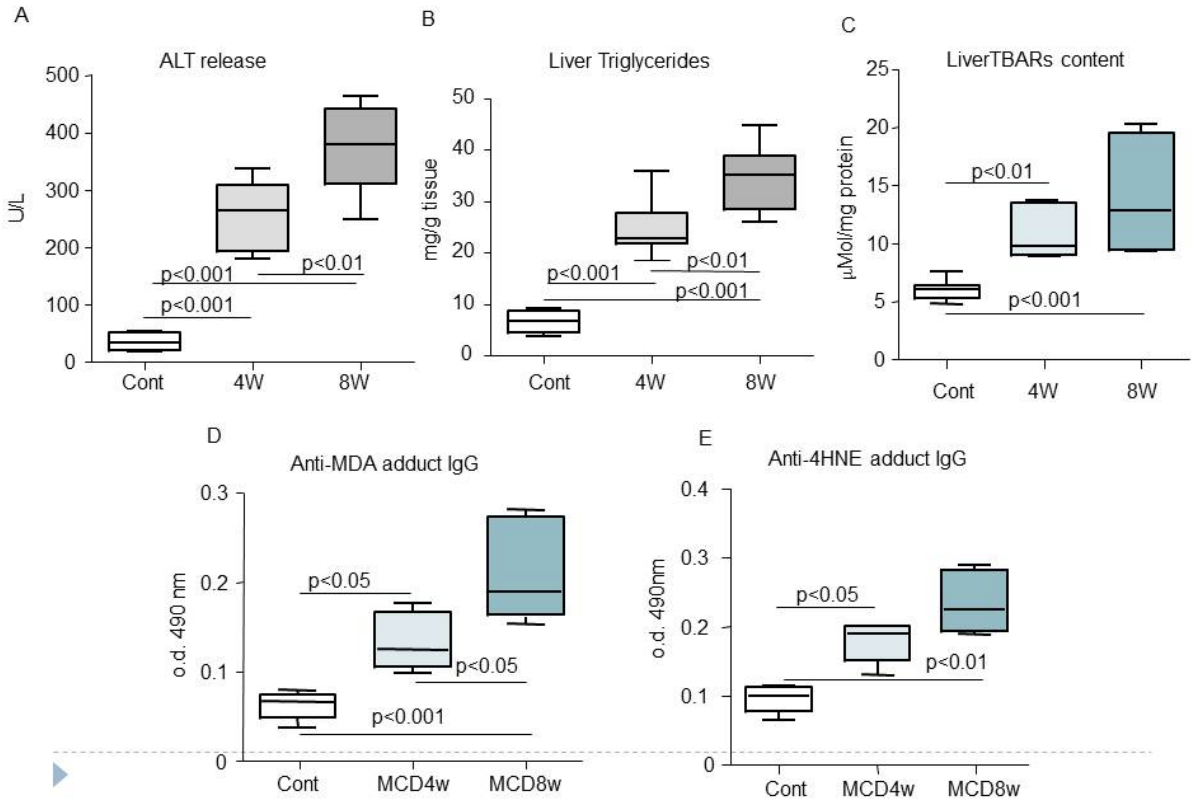

Figure 1 – Liver pathology of C57BL/6 mice fed by methionine/choline deficient (MCD) diet.

Panels A-C: Liver damage was measured by alanine aminotransferase (ALT) release and hepatic triglyceride content. Panels D-E: Liver oxidative stress, as evaluated by thiobarbituric acid reactive compounds (TBARs), and circulating IgG against malondialdehyde- (MDA) or 4-hydroxynonenal (4-HNE) modified bovine serum albumin were measured in control mice (empty bars) or in mice fed with the MCD diet for 4 (light grey bars) and 8 (dark grey bars) weeks. The IgG values are expressed as optical density at 490 nm. The values refer to 8-12 animals in each group and the boxes include the values within 25th and 75th percentile, while the horizontal bars represent the medians. The extremities of the vertical bars (10th-90th percentile) comprise the eighty percent of the values.

Figure 2

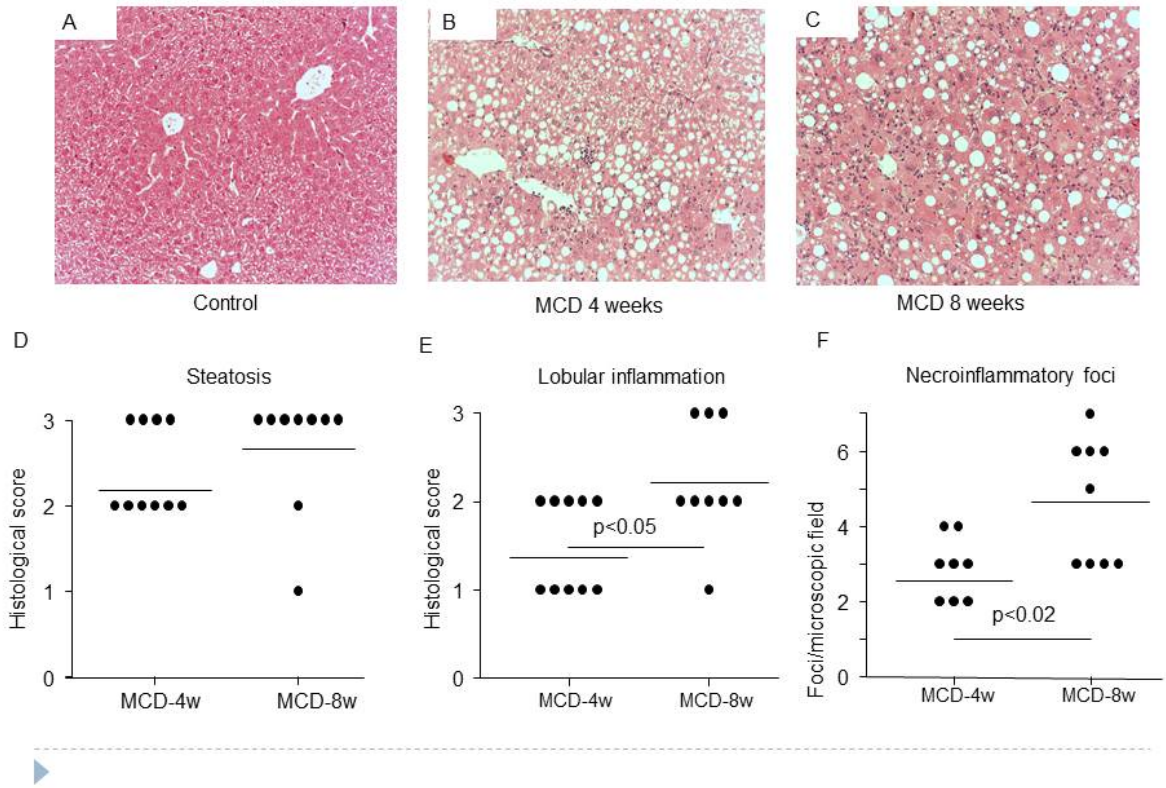

Figure 2 – Histological examination of hepatic environment in 4 and 8 weeks MCD diet fed mice.

Panels A-F: Liver histology was evaluated in hematoxilin/eosin stained sections from control mice to 4 and 8 weeks MCD-fed mice (magnification 400x). Lobular inflammation was scored according to Kleiner et al. [29], while necro-inflammatory foci and apoptotic hepatocytes were counted in ten different high magnification microscopic fields.

Figure 3 – Differential lymphocyte infiltration in hepatic environment in 4-8 weeks of MCD diet.

Panel A-B: Liver histology was evaluated in hematoxilin/eosin stained sections from mice receiving anti-CD3 and CD220 IgG or vehicle (magnification 400x). Panel C-F: Flow cytometry analysis of liver monucleated cells isolated from controls (Cont) or MCD-fed mice: representative dot blots of T-lymphocyte staining for CD45 and CD3 and percent distribution of total CD3+, CD8+ or CD4+ T-cells. The values refer to 4-5 animals in each group and the bars represent medians ± S.D. T-lymphocyte activation in NASH livers (8 weeks MCD diet) was assessed by CD3+ T-cell expression of CD69 as well as by CD4+ T-cell interferon-γ (IFN-γ) production.

Figure 3

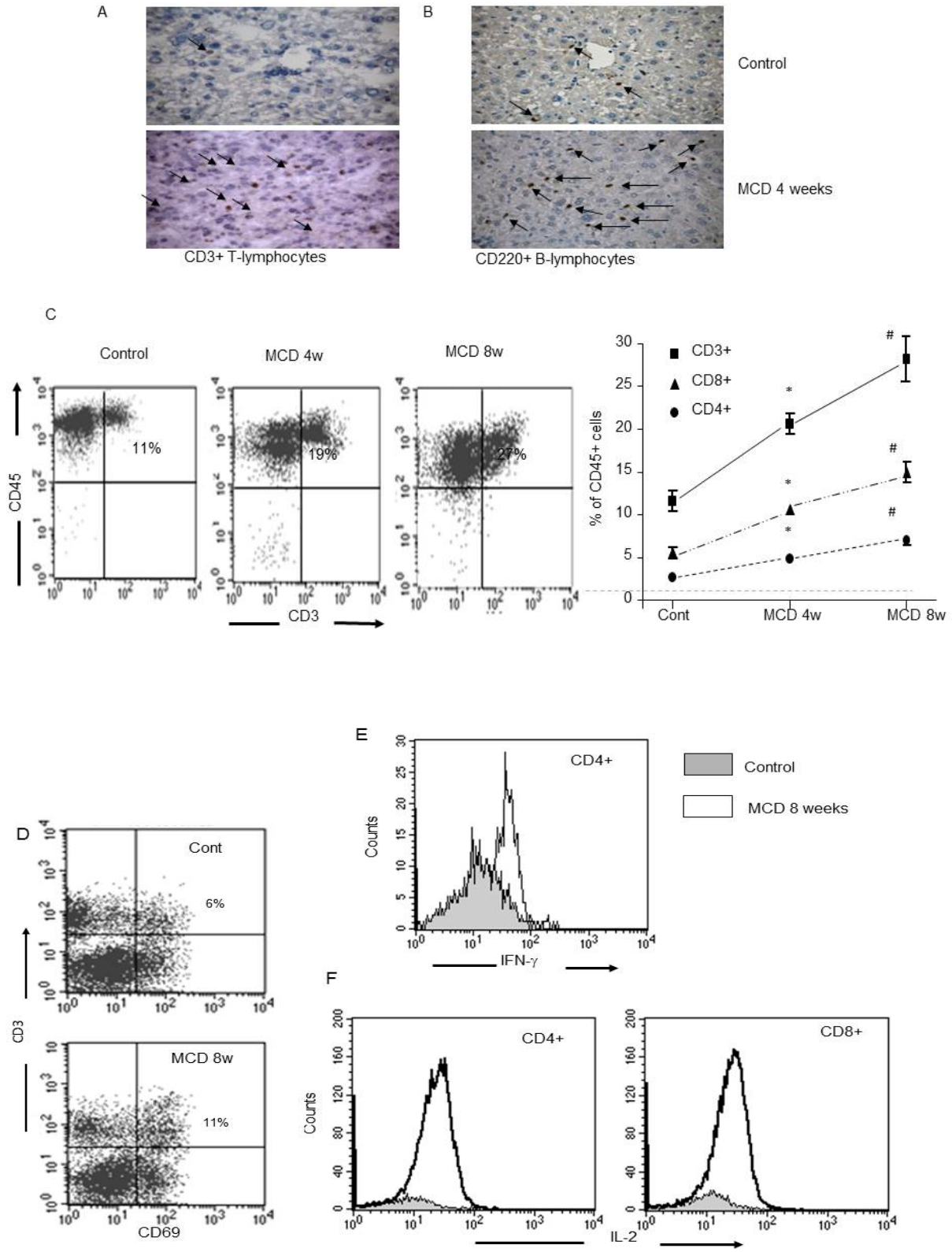
A
B
Control
MCD 4 weeks
CD3+ T-lymphocytes
CD220+ B-lymphocytes
C
Control
MCD 4w
MCD 8w
CD45
CD3
11%
19%
27%
CD3+
CD8+
CD4+
% of CD45+ cells
Cont
MCD 4w
MCD 8w
D
Cont
6%
MCD 8w
11%
CD3
CD69
E
CD4+
Control
MCD 8 weeks
Counts
IFN-γ
F
CD4+
CD8+
Counts
IL-2

Figure 4

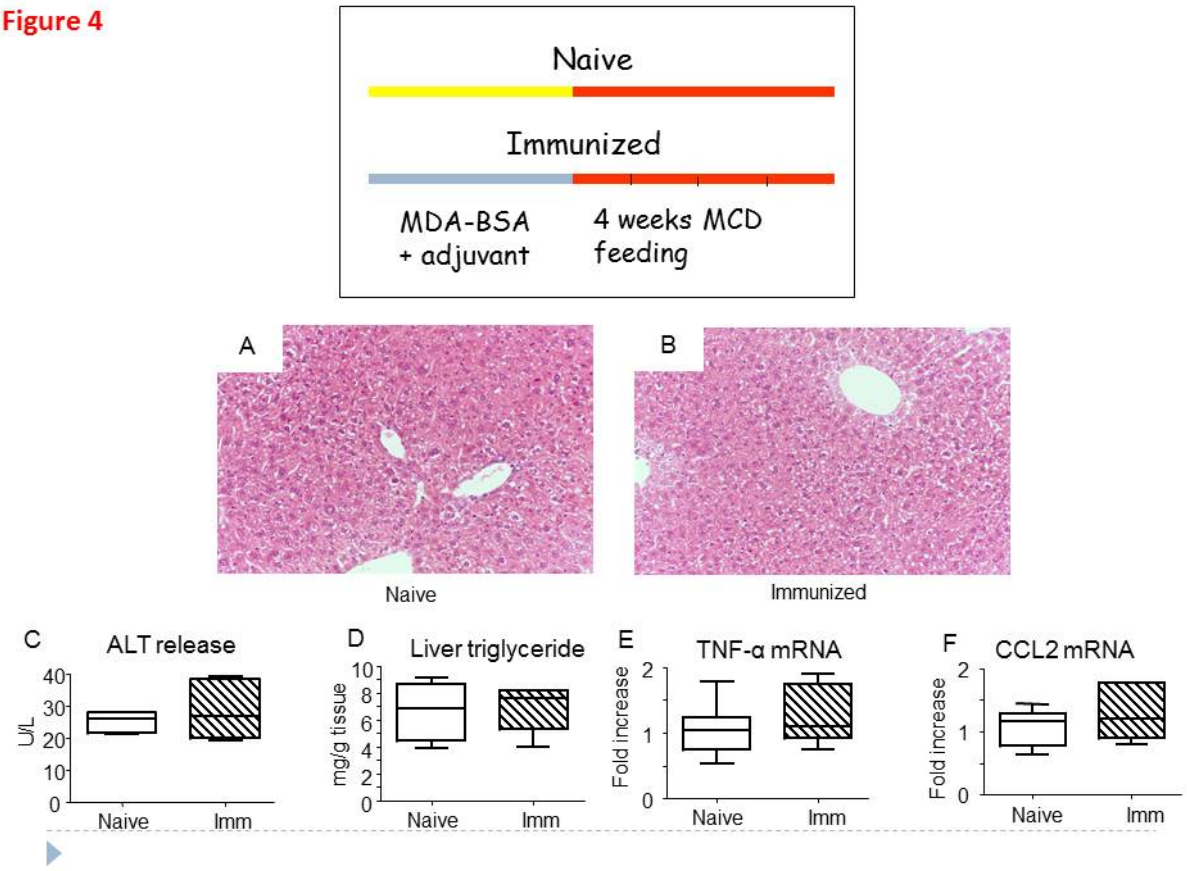

Figure 4 – MDA-BSA/adjuvant immunization does not affect the physiology in naïve mice with control diet.

Panel A-B: Liver histology of naïve and immunized mice on control diet was evaluated in hematoxilin/eosin stained sections from naïve or immunized control diet fed animals (magnification 400x). Panel C-F: Liver damage was measured by alanine aminotransferase (ALT) release, hepatic triglyceride content and liver mRNA levels for TNF-α, CCL2. Hepatic mRNAs were measured by RT-PCR and expressed as fold increase over control values after normalization to the β-actin gene expression. The values refer to 8-12 animals in each group and the boxes include the values within 25th and 75th percentile, while the horizontal bars represent the medians. The extremities of the vertical bars (10th-90th percentile) comprise the eighty percent of the values.

Figure 5

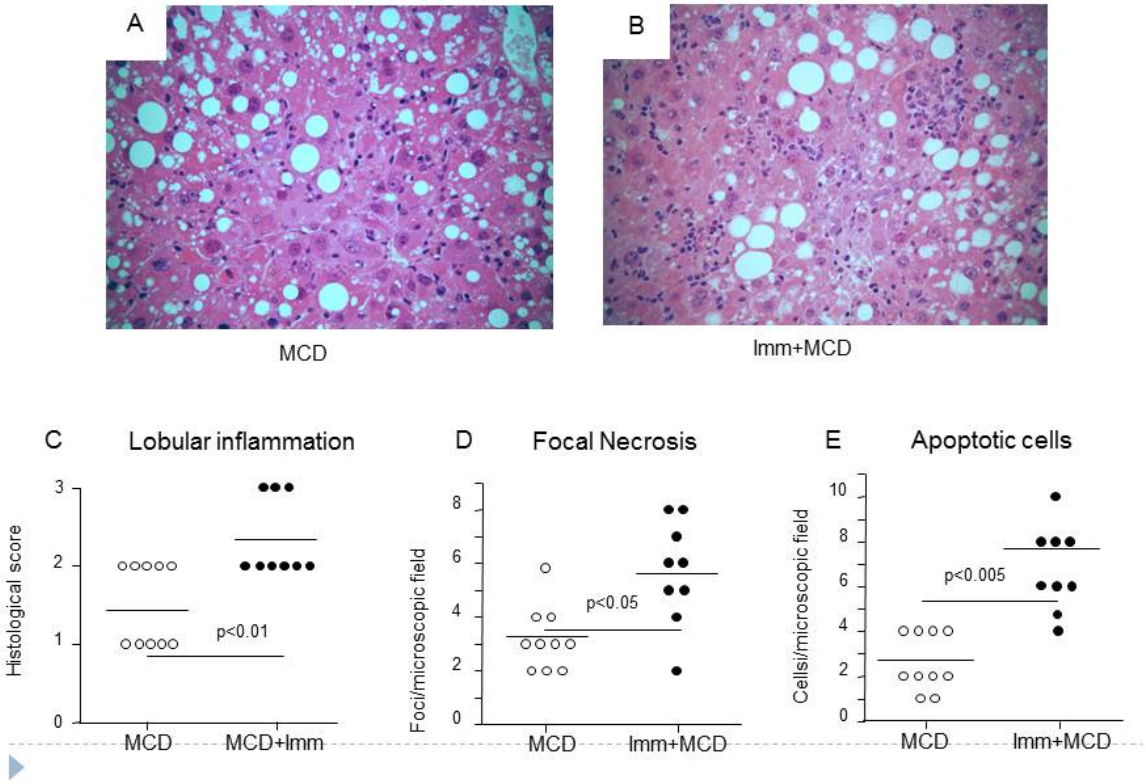

Figure 5 – Effects of immunization on the severity of NASH in MCD fed mice.

Mice were immunized with MDA-modified bovine serum albumin (MDA-BSA) in incomplete Freund's adjuvant before 4 weeks feeding with the MCD diet. Panels A-E: Liver histology of naïve and immunized mice on control diet was evaluated in hematoxilin/eosin stained sections from naïve (MCD) or pre-immunized MCD-fed animals (Imm-MCD) (magnification 400x). Lobular inflammation was scored according to Kleiner et al. [29], while necro-inflammatory foci and apoptotic hepatocytes were counted in ten different high magnification microscopic fields.

Figure 6

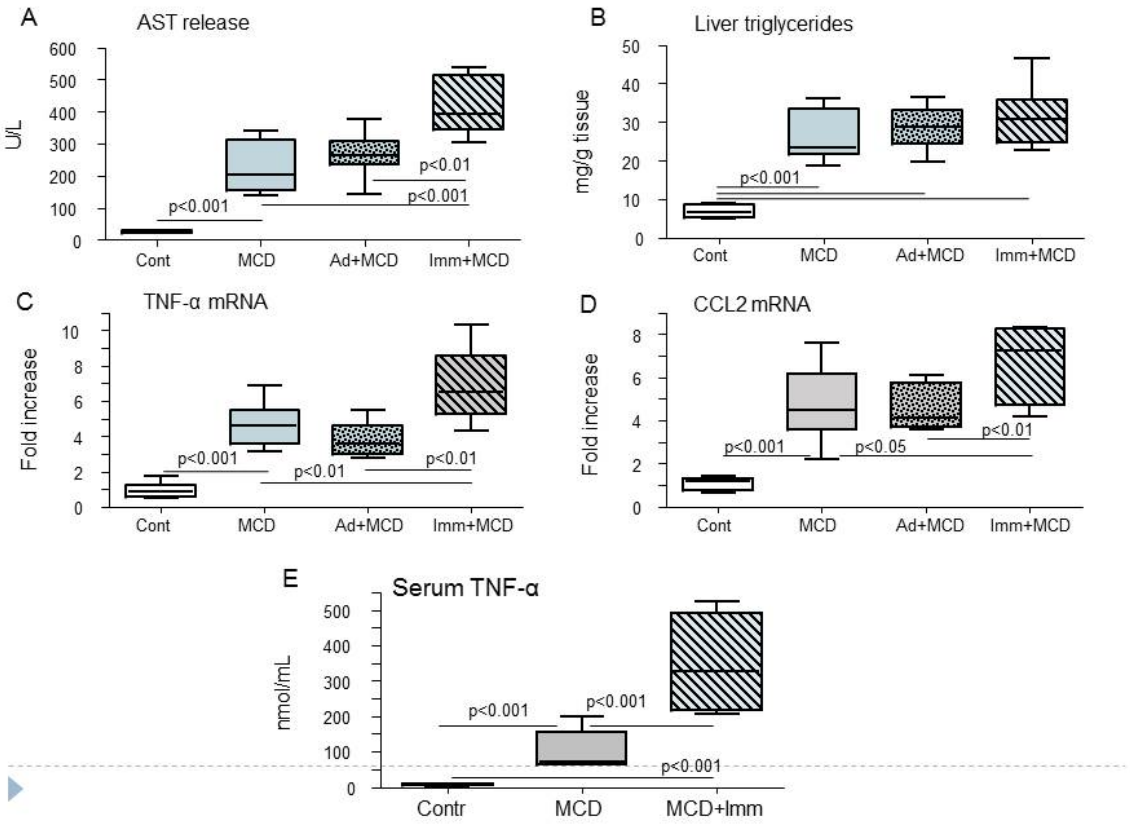

Figure 6 – Immunization affects the degree of severity in MCD diet induced liver damage

Mice were immunized with MDA-modified bovine serum albumin (MDA-BSA) in incomplete Freund's adjuvant before 4 weeks feeding with the MCD diet. Panels A-E: The differences in NASH severity were assessed by alanine aminotransferase (ALT) release, hepatic triglyceride content and liver mRNA levels for TNF-α, CCL2. The experimental groups were: naïve controls (Cont), naïve MCD-fed mice (MCD), mice pretreated with the incomplete Freund's adjuvant and receiving the MCD diet (Ad+MCD), mice receiving the complete immunization protocol plus the MCD diet (Imm-MCD). Panel E: Circulating TNF-α levels were determined in the same animals. Hepatic mRNAs were measured by RT-PCR and expressed as fold increase over control values after normalization to the β-actin gene expression. The values refer to 8-12 animals in each group and the boxes include the values within 25th and 75th percentile, while the horizontal bars represent the medians. The extremities of the vertical bars (10th-90th percentile) comprise the eighty percent of the values.

Figure 7

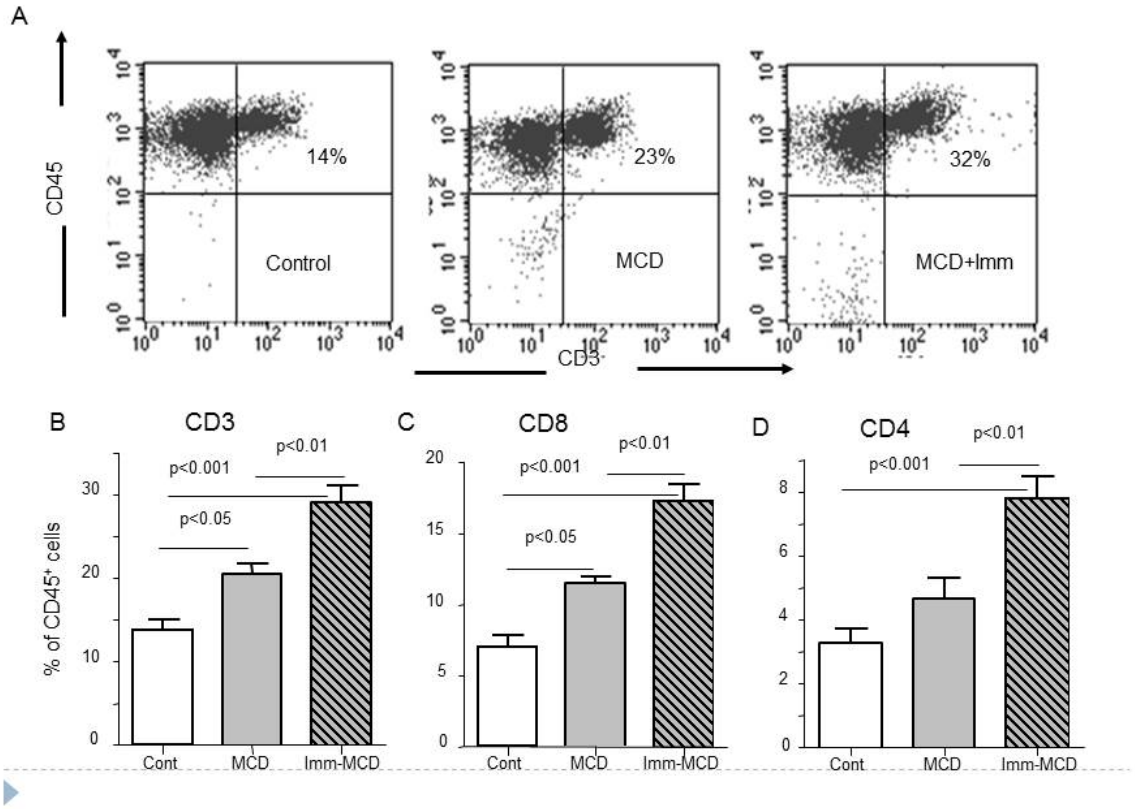

Figure 7 – The immune responses against oxidative stress-derived antigens promote the liver recruitment of T-lymphocytes.

Liver monucleated cells were isolated from the livers of either naive controls (Cont), naïve mice fed 4 weeks a methionine-choline deficient (MCD) diet or mice pre-immunized with MDA-modified bovine serum albumin before the administration of the MCD diet (Imm-MCD). Panels A-D show representative dot blots of T-lymphocytes staining for CD45 and CD3 and the percent distribution of total CD3+ and CD8+ or CD4+ T-cells sub-sets. The values refer to 5-6 animals in each group and the bars represent medians ± S.D.

Figure 8

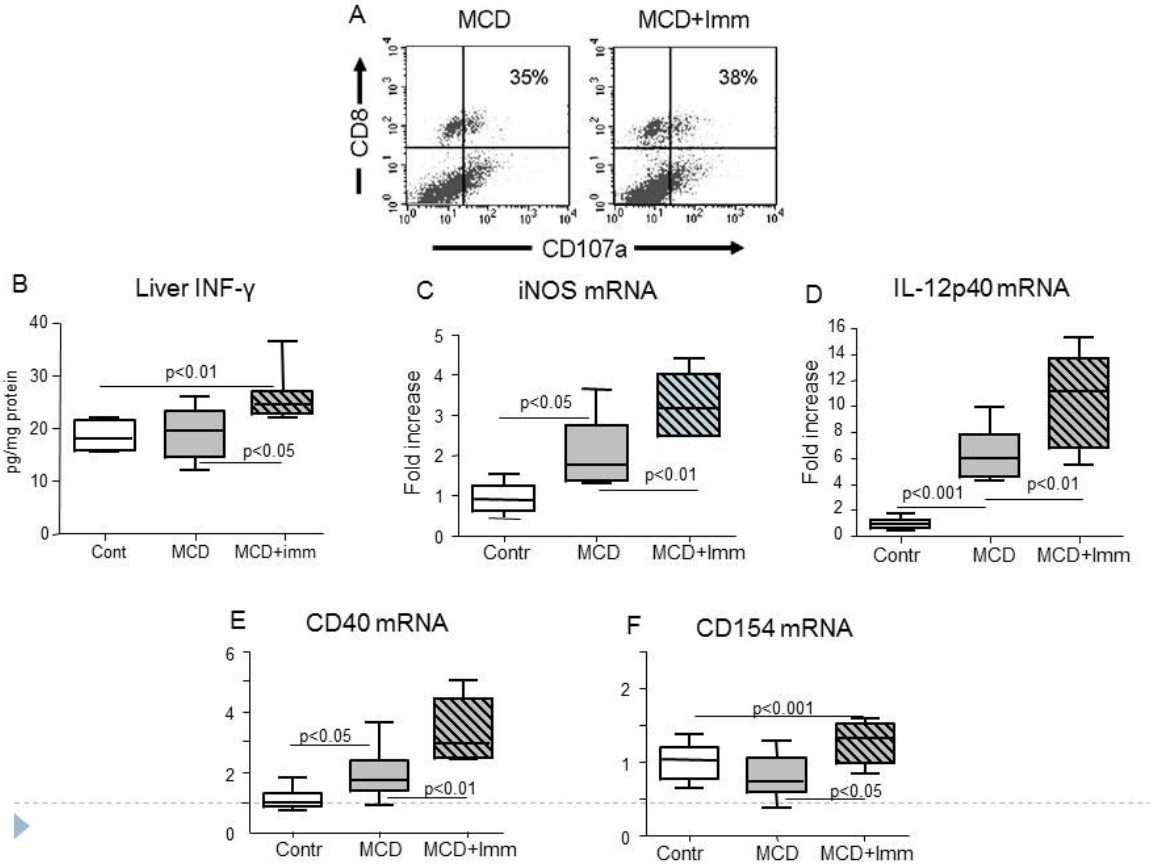

Figure 8 – Th-1 related immune responses during lymphocytes infiltration.

Panel A: Representative dot blots of CD8+ T-cells displaying the CD107b activation marker. Panels B-F: Th-1 activation of CD4+ T-cells was evidenced by the intrahepatic production of interferon-γ (IFN-γ) and the mRNA expression of the Th-1 trascription factor CD40 and CD40 ligand (CD154) and M1 activation marker iNOS. The RT-PCR values were normalized to those of the β-actin gene and presented as fold increase over control values. The data refer to 8-12 animals in each group and the boxes include the values within 25th and 75th percentile, while the horizontal bars represent the medians. The extremities of the vertical bars (10th-90th percentile) comprise the eighty percent of the values.

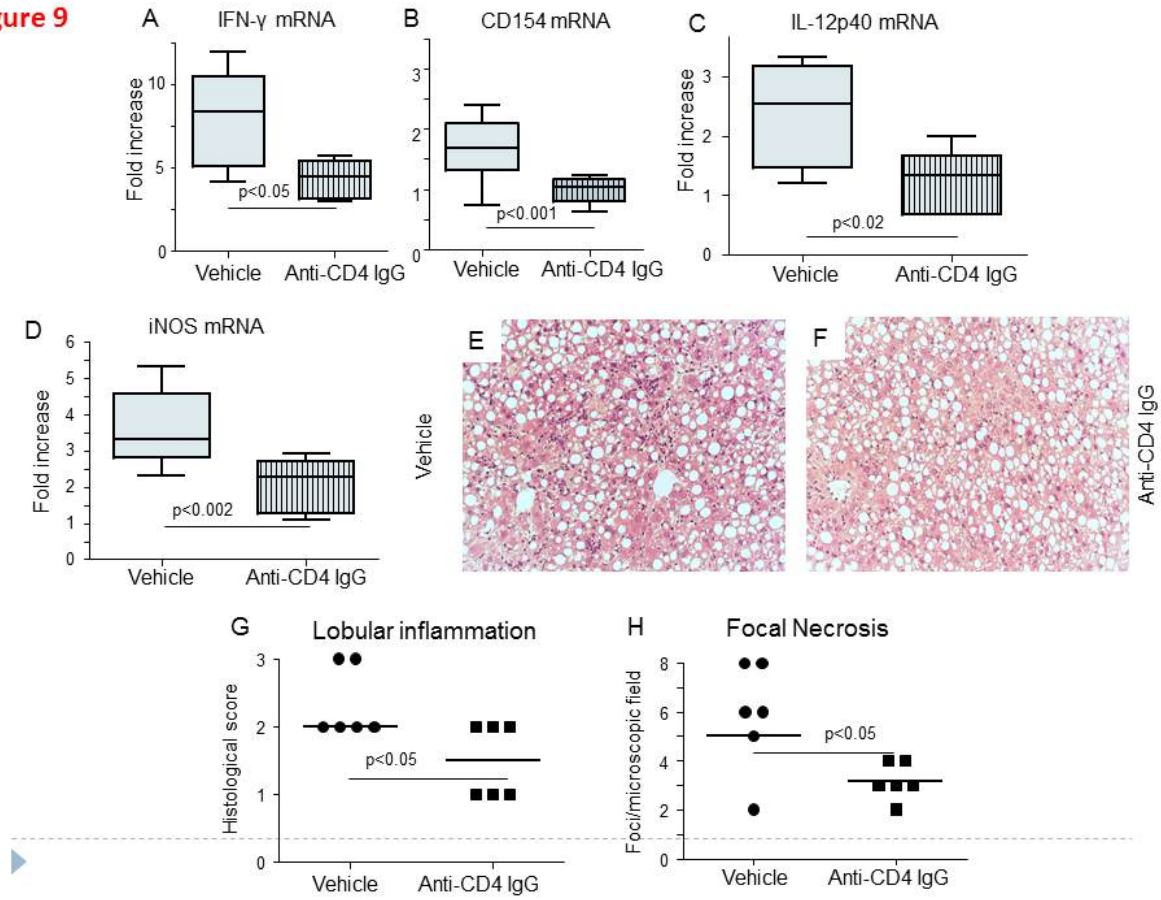

Figure 9 – CD4+ T-lymphocyte depletion improves hepatic inflammation in MDA-BSA immunized mice receiving the MCD diet.

After immunization with MDA-modified bovine serum albumin (MDA-BSA) mice were depleted of CD4+ T-cells by repeated injection of GK1.5 anti-CD4 monoclonal antibodies during 4 weeks feeding with the MCD diet. Panels A-D: Effect of CD4+ T-cell depletion on the hepatic expression of interferon-γ (IFN-γ), CD40 ligand (CD154), macrophage M1 activation markers (IL-12p40, iNOS). The mRNA levels were measured by RT-PCR and expressed as fold increase over control values after normalization to the β-actin gene expression. The values refer to 6 animals in each group and the boxes include the values within 25th and 75th percentile, while the horizontal bars represent the medians. The extremities of the vertical bars (10th-90th percentile) comprise the eighty percent of the values. Panels E-H: Liver histology was evaluated in hematoxilin/eosin stained sections from mice receiving anti-CD4 IgG or vehicle (magnification 400x). Lobular inflammation was scored according to Kleiner et al. [29] while necro-inflammatory foci were counted in ten different high magnification microscopic fields.

References

1. Angulo P, Lindor KD (2002) Non-alcoholic fatty liver disease. J Gastroenterol Hepatol 17 Suppl: S186-190.

2. Brunt EM (2001) Nonalcoholic steatohepatitis: definition and pathology. Semin Liver Dis 21: 3-16.

3. Denhardt DT, Giachelli CM, Rittling SR (2001) Role of osteopontin in cellular signaling and toxicant injury. Annu Rev Pharmacol Toxicol 41: 723-749.

4. Felga G, Evangelista AS, Salvalaggio PR, Curvelo LA, Della Guardia B, et al. (2012) Hepatocellular carcinoma recurrence among liver transplant recipients within the Milan criteria. Transplant Proc 44: 2459-2461.

5. Marion AW, Baker AJ, Dhawan A (2004) Fatty liver disease in children. Arch Dis Child 89: 648-652.

6. Roheim PS, Biempica L, Edelstein D, Kosower NS (1971) Mechanism of fatty liver development and hyperlipemia in rats treated with allylisopropylacetamide. J Lipid Res 12: 76-83.

7. Topping DL, Turner DM (1975) Plasma triglyceride secretion in squirrel monkeys: effects of nicotine. Nutr Metab 18: 89-98.

8. Gordon GB (1977) Lipid accumulation in the stationary phase of strain L cells in suspension culture. Lab Invest 36: 114-121.

9. Khanna A, Guo M, Mehra M, Royal W, 3rd (2013) Inflammation and oxidative stress induced by cigarette smoke in Lewis rat brains. J Neuroimmunol 254: 69-75.

10. Bichet C, Cornet S, Larcombe S, Sorci G (2012) Experimental inhibition of nitric oxide increases Plasmodium relictum (lineage SGS1) parasitaemia. Exp Parasitol 132: 417-423.

11. Hossain N, Stepanova M, Afendy A, Nader F, Younossi Y, et al. (2011) Non-alcoholic steatohepatitis (NASH) in patients with polycystic ovarian syndrome (PCOS). Scand J Gastroenterol 46: 479-484.

12. Balmer ML, Dufour JF (2011) [Non-alcoholic steatohepatitis - from NAFLD to MAFLD]. Ther Umsch 68: 183-188.

13. Harmon RC, Tiniakos DG, Argo CK (2011) Inflammation in nonalcoholic steatohepatitis. Expert Rev Gastroenterol Hepatol 5: 189-200.

14. Carulli L, Ballestri S, Lonardo A, Lami F, Violi E, et al. (2013) Is nonalcoholic steatohepatitis associated with a high-though-normal thyroid stimulating hormone level and lower cholesterol levels? Intern Emerg Med 8: 297-305.

15. Hulek P, Dresslerova I (2011) [Steatosis and steatohepatitis in diabetic patient]. Vnitr Lek 57: 364-367.

16. Jung Y, Diehl AM (2010) Non-alcoholic steatohepatitis pathogenesis: role of repair in regulating the disease progression. Dig Dis 28: 225-228.

17. Bechmann LP, Gieseler RK, Sowa JP, Kahraman A, Erhard J, et al. (2010) Apoptosis is associated with CD36/fatty acid translocase upregulation in non-alcoholic steatohepatitis. Liver Int 30: 850-859.

18. Aghazadeh S, Amini R, Yazdanparast R, Ghaffari SH (2011) Anti-apoptotic and anti-inflammatory effects of Silybum marianum in treatment of experimental steatohepatitis. Exp Toxicol Pathol 63: 569-574.

19. Adams LA, Feldstein AE (2010) Nonalcoholic steatohepatitis: risk factors and diagnosis. Expert Rev Gastroenterol Hepatol 4: 623-635.

20. Brunt EM, Tiniakos DG (2010) Histopathology of nonalcoholic fatty liver disease. World J Gastroenterol 16: 5286-5296.

21. Fierbinteanu-Braticevici C, Dina I, Petrisor A, Tribus L, Negreanu L, et al. (2010) Noninvasive investigations for non alcoholic fatty liver disease and liver fibrosis. World J Gastroenterol 16: 4784-4791.

22. Shieh YS, Chang YS, Hong JR, Chen LJ, Jou LK, et al. (2010) Increase of hepatic fat accumulation by liver specific expression of Hepatitis B virus X protein in zebrafish. Biochim Biophys Acta 1801: 721-730.

23. Jaskiewicz K, Rzepko R, Sledzinski Z (2008) Fibrogenesis in fatty liver associated with obesity and diabetes mellitus type 2. Dig Dis Sci 53: 785-788.

24. Ito S, Yukawa T, Uetake S, Yamauchi M (2007) Serum intercellular adhesion molecule-1 in patients with nonalcoholic steatohepatitis: comparison with alcoholic hepatitis. Alcohol Clin Exp Res 31: S83-87.

25. Yang YY, Huang YT, Tsai TH, Hou MC, Lee FY, et al. (2012) Kupffer cell depletion attenuates leptin-mediated methoxamine-stimulated portal perfusion pressure and thromboxane A2 release in a rodent model of NASH-cirrhosis. Clin Sci (Lond) 123: 669-680.

26. Thomas A, Stevens AP, Klein MS, Hellerbrand C, Dettmer K, et al. (2012) Early changes in the liver-soluble proteome from mice fed a nonalcoholic steatohepatitis inducing diet. Proteomics 12: 1437-1451.

27. Nobili V, Parola M, Alisi A, Marra F, Piemonte F, et al. (2010) Oxidative stress parameters in paediatric non-alcoholic fatty liver disease. Int J Mol Med 26: 471-476.

28. Rolla R, Vidali M, Serino R, Pergolini P, Albano E, et al. (2007) Antibodies against oxidized phospholipids in laboratory tests exploring lupus anti-coagulant activity. Clin Exp Immunol 149: 63-69.

29. Kleiner DE, Brunt EM, Van Natta M, Behling C, Contos MJ, et al. (2005) Design and validation of a histological scoring system for nonalcoholic fatty liver disease. Hepatology 41: 1313-1321.

30. Locatelli I, Sutti S, Vacchiano M, Bozzola C, Albano E (2013) NF-kappaB1 deficiency stimulates the progression of non-alcoholic steatohepatitis (NASH) in mice by promoting NKT-cell-mediated responses. Clin Sci (Lond) 124: 279-287.

31. Nomura LE, Walker JM, Maecker HT (2000) Optimization of whole blood antigen-specific cytokine assays for CD4(+) T cells. Cytometry 40: 60-68.

32. Larter CZ, Yeh MM (2008) Animal models of NASH: getting both pathology and metabolic context right. J Gastroenterol Hepatol 23: 1635-1648.

33. Suttles J, Stout RD (2009) Macrophage CD40 signaling: a pivotal regulator of disease protection and pathogenesis. Semin Immunol 21: 257-264.

34. Kaminski DA, Randall TD (2010) Adaptive immunity and adipose tissue biology. Trends Immunol 31: 384-390.

35. Chatzigeorgiou A, Karalis KP, Bornstein SR, Chavakis T (2012) Lymphocytes in obesity-related adipose tissue inflammation. Diabetologia 55: 2583-2592.

36. Brunt EM (2010) Pathology of nonalcoholic fatty liver disease. Nat Rev Gastroenterol Hepatol 7: 195-203.

37. Kurien BT, Scofield RH (2008) Autoimmunity and oxidatively modified autoantigens. Autoimmun Rev 7: 567-573.

38. Bieghs V, van Gorp PJ, Walenbergh SM, Gijbels MJ, Verheyen F, et al. (2012) Specific immunization strategies against oxidized low-density lipoprotein: a novel way to reduce nonalcoholic steatohepatitis in mice. Hepatology 56: 894-903.

39. Walenbergh SM, Koek GH, Bieghs V, Shiri-Sverdlov R (2013) Non-alcoholic steatohepatitis: the role of oxidized low-density lipoproteins. J Hepatol 58: 801-810.

40. Hansson GK, Libby P (2006) The immune response in atherosclerosis: a double-edged sword. Nat Rev Immunol 6: 508-519.

41. Poggi M, Engel D, Christ A, Beckers L, Wijnands E, et al. (2011) CD40L deficiency ameliorates adipose tissue inflammation and metabolic manifestations of obesity in mice. Arterioscler Thromb Vasc Biol 31: 2251-2260.

42. Inzaugarat ME, Ferreyra Solari NE, Billordo LA, Abecasis R, Gadano AC, et al. (2011) Altered phenotype and functionality of circulating immune cells characterize adult patients with nonalcoholic steatohepatitis. J Clin Immunol 31: 1120-1130.

43. Novobrantseva TI, Majeau GR, Amatucci A, Kogan S, Brenner I, et al. (2005) Attenuated liver fibrosis in the absence of B cells. J Clin Invest 115: 3072-3082.

44. Dhirapong A, Lleo A, Yang GX, Tsuneyama K, Dunn R, et al. (2011) B cell depletion therapy exacerbates murine primary biliary cirrhosis. Hepatology 53: 527-535.

Seminars Attended

1. "Searching for novel genes and microRNAs inducing myocardial protection and regeneration" – Dr. Mauro Giacca – 20 November 2012 – Director of International Centre for Genetic Engineering and Biotechnology, Università di Trieste.

2. "Drosophila as a Model System for Biomedical Research" – Prof. Dirk Bohmann – 5 Dicembre 2012 – Department of Biomedical Genetics, University of Rochester Medical Center, Rochester, NY (USA).

3. "The Nrf2 transcription factor in disease, aging and stem cell function" – Prof. Dirk Bohmann – 7 Dicembre 2012 – Department of Biomedical Genetics, University of Rochester Medical Center, Rochester, NY (USA).

4. "Alumina/Zirconia composites for hip joint applications" – Dr. Alessandro Alan Porporati– 6 Marzo 2013 – Manager of Scientific Affairs, Medical Products Division, Ceramtec GmbH, Italy.

5. "Long non-coding RNAs and a typical protein-coding genes as new players in the regulation of neuronal functions" – Dr. Silvia Zucchelli – 14 Marzo 2013 - neo RTD BIO18 (genetics) of the Department of Health Sciences, Italy.

6. "Glioblastoma stem cell biology and its implications in cancer therapy" – Dr. Giuliana Pelicci– 22 Aprile 2013 – Department of Experimental Oncology, European Institute of Oncology, Milan, Italy.

7. "Carbapenemases: a last frontier for beta-lactam antibiotics?" – Prof. Giuseppe Cornaglia – 3 Maggio 2013 – Dipartimento di Patologia e Diagnostica Università degli studi di Verona, Italy.

8. "Red blood cells as carriers for magnetically targeted delivery of drugs" – Prof. Dr. Hans Bäumler – 24 Maggio 2013 - Berlin-Brandenburg Center for Regenerative Therapies, Charité – Universitätsmedizin Berlin.

9. “Skin cancer in vivo models, what they have and can tell us” – Dott. Girish Patel – 6 Giugno 2013 – School of Medicine, Cardiff University, United Kingdom.

10. “Stem/progenitor cell transplantation in the rat: A powerful tool to study tissue replacement in the normal and diseased liver” – Michael Oertel – 12 July 2013 – School of Medicine,Dept. of Pathology, University of Pittsburgh (USA).

Conferences Attended

1. EUROPEAN ASSOCIATION FOR THE STUDY OF LIVER 2013 – Amsterdam, 24-28 April 2013.

2. WORKSHOP AUTOANTIBODIES – Novara, 21-22 March 2013

Posters Presented

1. ANNEXIN A1 MODULATES THE PROGRESSION OF NONALCOHOLIC STEATOHEPATITIS (NASH) IN MICE. I. Locatelli, S. Sutti, A. Jindal, M. Vacchiano, C. Bozzola, S. Bena, S. McArthur, M. Perretti, E. Albano. 7th International Conference on ANNEXINS. 9th-11th September 2013. London (UK)

2. IMMUNE RESPONSES TRIGGERED BY OXIDATIVE STRESS CONTRIBUTE TO HEPATIC INFLAMMATION IN NONALCOHOLIC STEATO-HEPATITIS (NASH). S. Sutti, I Locatelli, A. Jindal, M. Vacchiano, C. Bozzola, E. Albano. EUROPEAN ASSOCIATION FOR THE STUDY OF THE LIVER APRIL 24-28, 2013 AMSTERDAM, NETHERLANDS JOURNAL OF HEPATOLOGY, VOL. 58, SUPPL 1 APRIL 2013

3. MACROPHAGE EXPRESSION OF ANNEXIN A1 CHARACTERIZES THE PROGRESSION OF NONALCOHOLIC STEATOHEPATITIS (NASH) IN MICE. I Locatelli, S. Sutti, A Jindal, M. Vacchiano, C. Bozzola, E. Albano. EUROPEAN ASSOCIATION FOR THE STUDY OF THE LIVER APRIL 24-28, 2013 AMSTERDAM, NETHERLANDS JOURNAL OF HEPATOLOGY, VOL. 58, SUPPL 1 APRIL 2013

4. COMPLEX ROLE OF OSTEOPONTIN IN THE PROGRESSION OF NONALCOHOLIC STEATOHEPATITIS (NASH). A Jindal, S. Sutti, I. Locatelli, A Chiocchetti, M.F. Soluri, M. Vacchiano, E Maldi, C. Bozzola, U. Dianzani, E. Albano. EUROPEAN ASSOCIATION FOR THE STUDY OF THE LIVER APRIL 24-28, 2013 AMSTERDAM, NETHERLANDS JOURNAL OF HEPATOLOGY, VOL. 58, SUPPL 1 APRIL 2013

5. IMMUNE RESPONSES AGAINST OXIDATIVE STRESS-DERIVED ANTIGENS CONTRIBUTE TO HEPATIC INFL AMMATION IN NONALCOHOLIC STEATO-HEPATITIS (NASH). Sutti S, Locatelli I, Jindal A, Vacchiano M, Bozzola C, Albano E.

XXXI Meeting of the Italian Society of Pathology and Translational Medicine. Udine 12-15 September 2012, The American Journal of Pathology , September 2012, Vol 181, Suppl.